

Prediction of bridge flutter under a crosswind flow

Tan-Van Vu¹, Ho-Yeop Lee², Byung-Ho Choi³ and Hak-Eun Lee^{*2}

¹Faculty of Civil Engineering, Ho Chi Minh City University of Architecture, Vietnam

²School of Civil, Environmental and Architectural Engineering, Korea University, Seoul, Korea

³Department of Civil Engineering, Hanbat National University, Seoul, Korea

(Received July 14, 2012, Revised November 25, 2012, Accepted December 15, 2012)

Abstract. This paper presents a number of approximated analytical formulations for the flutter analysis of long-span bridges using the so-called uncoupled flutter derivatives. The formulae have been developed from the simplified framework of a bimodal coupled flutter problem. As a result, the proposed method represents an extension of Selberg's empirical formula to generic bridge sections, which may be prone to one of the aeroelastic instability such as coupled-mode or single-mode (either dominated by torsion or heaving mode) flutter. Two approximated expressions for the flutter derivatives are required so that only the experimental flutter derivatives of (H_1^*, A_2^*) are measured to calculate the onset flutter. Based on asymptotic expansions of the flutter derivatives, a further simplified formula was derived to predict the critical wind speed of the cross section, which is prone to the coupled-mode flutter at large reduced wind speeds. The numerical results produced by the proposed formulas have been compared with results obtained by complex eigenvalue analysis and available approximated methods show that they seem to give satisfactory results for a wide range of study cases. Thus, these formulas can be used in the assessment of bridge flutter performance at the preliminary design stage.

Keywords: bridges; eigenvalue; flutter; flutter derivatives; selberg formula; simplified formulations

1. Introduction

A major consideration in the design stage of long-span bridges is the effect of wind on their overall performance since their slender, flexible and low damping characteristics renders them very susceptible to wind-induced vibrations. Among the wind-induced phenomena, flutter is one of the most critical mechanisms that could have an untoward affect on the bridge performance. Flutter is known as an aeroelastic instability phenomenon due to self-excited forces caused by wind-structure interactions, which may eventually lead to destructive forces on bridges, as was the case in the dramatic collapse of the Tacoma Narrows Bridge in 1940. Indeed, bridge flutter is highly dependent on the cross-sectional shape of the deck. Accordingly, coupled flutter or two degree-of-freedom flutter is often encountered in streamlined bridge sections, where flutter occurs from a coupling of simultaneous vertical and torsional motion of which the frequencies are in phase with one another. For a plate girder, and for several truss bridge sections, flutter occurs from a single degree-of-freedom (heaving-mode aeroelastic instability or torsional flutter), which was

*Corresponding author, Professor, E-mail: helee@korea.ac.kr

the cause of the 1826 damage to Telford's Menai Bridge as well as the wild oscillation of the Deer Isle Bridge in 1942 (Scott 2001). Flutter control and the evaluation method are major points of concern in the design of modern long-span bridges. At the preliminary design stage, not only the cross-section shape and external winglets or alterations of the bridge are optimized, but the bridge's inertial and dynamical parameters can also be changed so that the critical flutter wind speed of a bridge must transcend its design wind velocity. Consequently, a full aeroelastic model with chosen parameters is built to validate the design at the final design stage through a wind tunnel test campaign.

Since the experimental campaign is expensive and time-consuming, it could be very useful to propose an engineering tool that is able to quickly assess flutter performance based on the structural and aerodynamic parameters with the purpose of providing useful suggestions before starting the wind-tunnel tests. Regarding this context, the first pioneering research presented by Bleich (1948), wherein the bimodal coupled flutter considering fundamental vertical bending and torsional modes of bridge vibration, was performed by applying airfoil theory to model aerodynamic forces. Based on this theoretical foundation, Selberg (1961) and Rocard (1963) proposed empirical formulas that are able to quickly predict the flutter onset velocity, once the dynamical parameters are known. Due to their simplicity, these empirical formulas are still widely used as the engineering tool for bridge aerodynamic instability analysis at the preliminary design stage. Nevertheless, these empirical formulas can only be applied rigorously for a flat airfoil, though their use can be extended to real bridge cross-sections by employing empirical corrective factors (Dyrbye and Hansen 1997). Consequently, this may lead to under-estimated or over-estimated results. In order to overcome this disadvantage of the empirical formulas, a number of researchers have attempted to develop simplified formulations by means of the Selberg-type formula regarding the actual cross-section aerodynamic characteristic by using the experimental flutter derivatives (Scanlan and Tomko 1971). For example, Como *et al.* (2005) presented an approximated formula based on the quasi stationary assumption, wherein self-excited loads are described by an asymptotic expansion of flutter derivatives of (H_1^*, A_2^*, A_3^*) in the range of large values of the reduced velocity. Meanwhile, starting from closed-form formulations of the bimodal flutter problem, Chen and Kareem (2007) proposed simplified formulations, which are regarded as an analytical basis for Selberg's formula for bridges with generic bluff deck sections, wherein not only the coupled flutter derivatives (H_3^*, A_1^*) but also the uncoupled flutter derivatives (A_2^*, A_3^*) are included in order to analyze the flutter performance. Nevertheless, only the case of classical coupled flutter can be numerically validated by these approaches, and the Selberg-type formulas usually disregard the single degree-of-freedom flutter cases.

This work addresses the simplified framework for the bimodal bridge flutter problem that presented in Vu *et al.* (2011) with its further simplification concerning its robustness. With this goal, a formula remarkably similar to the Selberg formula for predicting the critical wind speed and frequency of a given bridge section that may be prone to coupled flutter or one degree-of-freedom flutter, is introduced in the second section of this paper.

Some further simplifications are proposed and discussed in the next section. The approximated expressions of uncoupled flutter derivatives of H_4^* and A_3^* are newly presented to reduce the number of experimental derivatives, which need to be identified from a spring-mounted bridge section model in a wind tunnel test. Based on the asymptotic expressions of uncoupled flutter derivatives, a simplified formula that calculates the critical wind speed for the cross sections prone to coupled flutter at large reduced wind speed is introduced.

Finally, in Section 4, several case studies are widely employed as benchmarks and ideal and existing cable-stayed bridges are discussed for addressing the influences of both structural parameters and bridge deck aerodynamic characteristics on the bridge flutter. Comparisons with results obtained by the conventional complex eigenvalue analysis (CEA) and other formulations or available experimental evidences show the effectiveness and limitation of the proposed formulas.

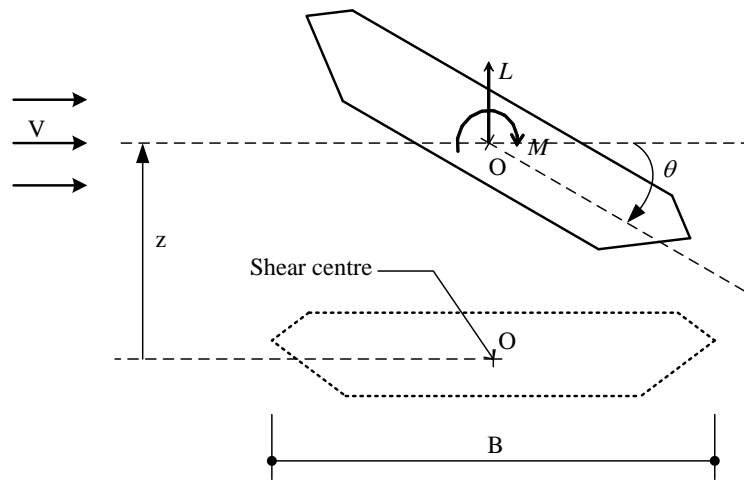


Fig. 1 Sign convention for the displacements and self-excited forces

2. Approximate solutions for bimodal flutter problem

In a framework of bimodal flutter analysis, the bridge deck is considered as a two-degree-of-freedom system undergoing vertical and torsional vibrations (Fig. 1), and the equations of motion can be written as follows

$$\tilde{m}_z \left[\ddot{z}(x,t) + \dot{z}(x,t) \zeta_z \omega_z + z(x,t) \omega_z^2 \right] = L_{se}(t) \tag{1}$$

$$\tilde{m}_\theta \left[\ddot{\theta}(x,t) + \dot{\theta}(x,t) \zeta_\theta \omega_\theta + \theta(x,t) \omega_\theta^2 \right] = M_{se}(t) \tag{2}$$

where $z(x,t), \theta(x,t)$ = vertical and torsion displacement; $\tilde{m}_z, \tilde{m}_\theta$ = mass and mass moment of inertia per unit length, respectively; ω_z, ω_θ = natural circular frequencies of vertical and torsional modes; ζ_z, ζ_θ = ratio-to-critical damping coefficients; and $L_{se}(t), M_{se}(t)$ = self-excited lift and pitching moment acting on the bridge deck section per unit length, given by (Simiu and Scanlan 1996)

$$L_{se}(t) = \frac{1}{2} \rho V^2 B \left[KH_1^* \frac{\dot{z}}{V} + KH_2^* \frac{B \dot{\theta}}{V} + K^2 H_3^* \theta + K^2 H_4^* \frac{z}{B} \right] \tag{3}$$

$$M_{se}(t) = \frac{1}{2} \rho V^2 B^2 \left[KA_1^* \frac{\dot{z}}{V} + KA_2^* \frac{B\dot{\theta}}{V} + K^2 A_3^* \theta + K^2 A_4^* \frac{z}{B} \right] \quad (4)$$

where V = mean wind speed, B = bridge deck, ρ = air density, ω = in-wind circular frequency; $K = 2k$ is the reduced frequency, and $H_i^*, A_i^* (i = \overline{1,4})$ = flutter derivatives that are functions of reduced frequency. Substituting Eqs. (3) and (4) into Eqs. (1) and (2) taking the Fourier transform, two flutter equations are then obtained by vanishing of the imaginary or real parts of the impedance matrix determinant (Strømmen 2006) as follows

$$I_1 \Omega^3 + I_2 \Omega^2 + I_3 \Omega + I_4 = 0 \quad (5)$$

$$R_1 \Omega^4 + R_2 \Omega^3 + R_3 \Omega^2 + 1 = 0 \quad (6)$$

in which the coefficients of the imaginary flutter equation are written as,

$$I_1 = \gamma^2 \left[0.5(\lambda_z H_1^* + \lambda_\theta A_2^*) + 0.25 \lambda_z \lambda_\theta C_I \right] \quad (7a)$$

$$I_2 = -2 \left[\zeta_z (0.5 \lambda_\theta A_3^* + \gamma) + \gamma^2 \zeta_\theta (0.5 \lambda_z H_4^* + 1) \right] \quad (7b)$$

$$I_3 = -0.5(\lambda_z \gamma^2 H_1^* + \lambda_\theta A_2^*) \quad (7c)$$

$$I_4 = 2(\zeta_z \gamma + \zeta_\theta) \quad (7d)$$

while the coefficients of the real flutter equation are given by

$$R_1 = \gamma^2 \left[1 + 0.5(\lambda_z H_4^* + \lambda_\theta A_3^*) + 0.25 \lambda_z \lambda_\theta C_R \right] \quad (8a)$$

$$R_2 = \gamma(\gamma \zeta_\theta \lambda_z H_1^* + \zeta_z \lambda_\theta A_2^*) \quad (8b)$$

$$R_3 = - \left[1 + \gamma^2 + 4\gamma \zeta_\theta \zeta_z + 0.5(\lambda_z \gamma^2 H_4^* + \lambda_\theta A_3^*) \right] \quad (8c)$$

where $C_I = H_1^* A_3^* - H_2^* A_4^* - H_3^* A_1^* + H_4^* A_2^*$, $C_R = A_1^* H_2^* - A_2^* H_1^* + A_3^* H_4^* - A_4^* H_3^*$; $\gamma = \omega_\theta / \omega_z$; is the structural frequency ratio; $\lambda_z = \rho B^2 / \tilde{m}_z$ and $\lambda_\theta = \rho B^4 / \tilde{m}_\theta$ represent the non-dimensional mass and the polar moment of inertia, respectively; and $\Omega = \omega / \omega_\theta$ is the in-wind frequency ratio. It can be seen that the solution of these equations requires searching for the lowest identical roots with respect to Ω from both the fourth and third degree polynomials.

From analysing dynamic and aerodynamic parameters from the basic section configurations including bluff girders, which are streamlined box and slotted girder sections that are widely used in the design of cable-supported bridges, Vu *et al.* (2011) reported that the terms I_2 , I_4 and R_2 combined with structural damping can be neglected with respect to the other terms as a good approximation. In addition, the coefficients of $0.25 \gamma^2 \lambda_z \lambda_\theta C_R$ and $0.25 \gamma^2 \lambda_z \lambda_\theta C_I$, associated with

coupled and uncoupled flutter, respectively, are also omitted in the R_I and I_I terms. With regard to this context, Eqs. (5) and (6) become more compacted as follows

$$\gamma^2 (\lambda_z H_1^* + \lambda_\theta A_2^*) \Omega^3 - (\lambda_z \gamma^2 H_1^* + \lambda_\theta A_2^*) \Omega = 0 \tag{9}$$

$$\gamma^2 [1 + 0.5 (\lambda_z H_4^* + \lambda_\theta A_3^*)] \Omega^4 - [1 + \gamma^2 + 4\gamma \zeta_\theta \zeta_z + 0.5 (\lambda_z \gamma^2 H_4^* + \lambda_\theta A_3^*)] \Omega^2 + 1 = 0 \tag{10}$$

Therefore, Eq. (9) can be used to find the critical frequency of the combined bridge system in the following way

$$\Omega = \frac{1}{\gamma} \sqrt{\frac{\lambda_z \gamma^2 H_1^* + \lambda_\theta A_2^*}{\lambda_z H_1^* + \lambda_\theta A_2^*}} \tag{11}$$

Substituting Eq. (11) into Eq. (10) and after rearranging a number of terms, it leads to a non-linear equation is used to calculate the critical reduced wind speed as follows

$$(1 - \gamma^2) \lambda_z \lambda_\theta [(H_1^* \lambda_z \gamma^2 + A_2^* \lambda_\theta) (A_3^* H_1^* - H_4^* A_2^*) + 2H_1^* A_2^* (1 - \gamma^2)] + 8\gamma \zeta_z \zeta_\theta (A_2^* \lambda_\theta + H_1^* \lambda_z \gamma^2) \times (A_2^* \lambda_\theta + H_1^* \lambda_z) = 0 \tag{12}$$

On the other hand, the relationship between the in-wind circle frequency and reduced wind speed can take the form of

$$\omega = \frac{VK}{B} \tag{13}$$

Substituting Eq. (13) into Eq. (11) leads to

$$(\lambda_z \gamma^2 H_1^* + \lambda_\theta A_2^*) = \gamma^2 (\lambda_z H_1^* + \lambda_\theta A_2^*) \frac{V^2 K^2}{B^2 \omega_\theta^2} \tag{14}$$

At this point, substituting Eq. (14) into Eq. (12), after rearranging the terms, we finally find

$$V = \omega_\theta B \chi \sqrt{\left(1 - \frac{1}{\gamma^2}\right) \frac{2}{(\lambda_z \lambda_\theta)^{0.5}}} \tag{15}$$

where

$$\chi = \sqrt{\frac{(\lambda_z \lambda_\theta)^{1.5} H_1^* A_2^* (\gamma^2 - 1)}{4k^2 (\lambda_z H_1^* + \lambda_\theta A_2^*) [(\gamma^2 - 1) \lambda_z \lambda_\theta (A_3^* H_1^* - A_2^* H_4^*) - 8\gamma \zeta_z \zeta_\theta (\lambda_z H_1^* + \lambda_\theta A_2^*)]}} \tag{16}$$

In addition, Eq. (14) can be rewritten as

$$V = \frac{B\omega_\theta}{K\gamma} \sqrt{\frac{\lambda_z \gamma^2 H_1^* + \lambda_\theta A_2^*}{\lambda_z H_1^* + \lambda_\theta A_2^*}} \tag{17}$$

The intersection of the curve obtained by Eqs. (15) and (17) as the functions of reduced frequency, K provides an approach for estimating the critical wind speed and frequency of a given

bridge deck. It can be observed that the form of Eq. (15) is similar to the empirical Selberg's formula and the simplified formulation proposed by Chen and Kareem. The parameter value of χ is constant as suggested by Selberg, while the value is a function of coupled and uncoupled flutter derivatives of A_2^*, H_3^*, A_1^* and A_3^* as proposed by Chen and Kareem. It is clear that only uncoupled flutter derivatives (H_1^*, H_4^*, A_2^* and A_3^*) are included in Eq. (16) to clarify whether a given bridge section is prone to coupled flutter or single degree-of-freedom type of flutter.

Table 1 Geometric and dynamics properties of the different bridges

	$B(m)$	$f_z(Hz)$	γ	$\zeta_z = \zeta_\theta$	$\tilde{m}_z \left(\frac{kg}{m} \right)$	$\tilde{m}_\theta \left(\frac{kgm^2}{m} \right)$	λ_z	λ_θ	$\beta = \lambda_z \lambda_\theta$
<i>Edge girder bridge section</i>									
Busan-Geoge	22.0	0.334	3.00	0.005	26,854	1,430,000	0.023	0.205	0.005
Seohae	34.0	0.250	1.84	0.005	28,789	2,756,000	0.050	0.606	0.030
Kärkinen	13.28	0.4646	1.51	0.0064	17,193	306,218	0.013	0.127	0.002
<i>Streamline bridge section</i>									
Great Belt	31.0	0.099	2.75	0.005	22,700	2,470,000	0.053	0.467	0.025
2nd Geo-Germ	16.9	0.185	2.99	0.003	11,699	295,250	0.031	0.345	0.011
Hoga Kusten	22.0	0.1198	2.10	0.005	10,588	603,209	0.057	0.485	0.028
<i>Slotted box girder bridge section</i>									
Messina									
Straits	60.4	0.0605	1.32	0.01	55,000	28,000,000	0.083	0.594	0.049
Xihoumen	36.0	0.1005	2.31	0.01	27,511	4,002,800	0.059	0.525	0.031
Shanghai	51.5	0.2520	2.64	0.005	35,151	10,076,000	0.094	0.873	0.082

Indeed, the main structural parameters affecting wind-induced critical states in long-span bridges are the dimensionless mass, polar moment of inertia ratios $\lambda_z, \lambda_\theta$, and the frequency ratio γ (Dyrbye and Hansen 1997). Hence, some geometric and dynamic properties from a variety of existing bridge decks are collected, with the aim of investigating the effectiveness of the proposed formulas. Table 1 summarizes the data of four edge girder bridge sections with dimensions and cross sections taken into account: Busan-Geoge (Lee *et al.* 2004), Seohae Grand (KHC 1998), and Kärkinen (Kiviluoma 2001). Data of the streamlined bridge sections is shown in the second part of Table 1: Great Belt (Larsen 1993, Nissen *et al.* 2004), 2nd Geo-Germ (Larsen 2002), and Hoga Kusten (Livesey 1995). At the bottom of the table, three slotted girder bridge sections are considered: Messina Straits (D'Asdia and Sepe 1998), Xihoumen (Yang *et al.* 2007) and Shanghai (Zhou and Ge 2009). From the data gathered in the last column of Table 1, it seems reasonable to consider that the Kärkinen and Shanghai bridges are typical cases, since their non-dimensional dynamic parameters are $\beta_1 = 0.002 (\lambda_z = 0.013, \lambda_\theta = 0.013)$ and $\beta_2 = 0.082 (\lambda_z = 0.094, \lambda_\theta = 0.873)$ as the smallest and highest values, respectively. These cases will be assumed as reference case studies in the following analyses.

Fig. 2 shows the corresponding parameter χ calculated by Eq. (16) and the available formulas for a typical flat plate (Theodorsen 1934, Fung 1993), in which the structural damping is neglected. Accordingly, assuming that the non-dimensional dynamic parameters β_1 with the reduced wind speed varied from 6 to 22, the proposed formula shows the values of χ decreasing from 0.418 to 0.412, which are close to the value of 0.416 as suggested by Selberg. Meanwhile, Chen and Kareem’s formula shows these values increasing from 0.402 to 0.420. It is observed that there is a slight increase of 1% in the values of χ when the value β_2 is assumed, and the proposed formula predicts the lowest critical wind speed for the section at which the range of reduced wind speed V/fB is larger than 9.

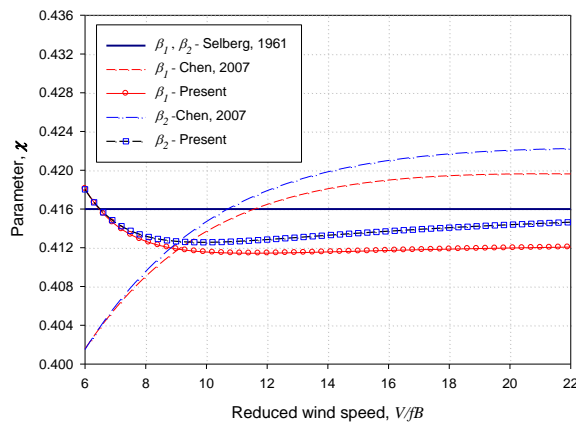


Fig. 3 Comparison of parameter χ for different deck section: (a) $\beta_1 = 0.002$ and (b) $\beta_2 = 0.082$

For an actual section, the flutter derivatives can be extracted from a spring-mounted bridge section model in a wind tunnel test, and the parameter χ can be used as a useful index for seeking a section shape having the superior aerodynamic characteristics among the design geometric shapes of cross sections. Accordingly, the higher value of the parameter χ shows a better flutter execution of the deck section shape. Fig. 3 shows that the slotted girder section *2TF* (Matsumoto 2004) exhibits the best flutter performance, while the bluffer rectangular section characterized by chord-to thickness ratios of *R15* (Matsumoto 1996) shows the worst flutter performance at all the investigated deck cross-sections having the same structural dynamic properties. A good agreement in predicting the flutter onset between Approx. 1 [Eqs. (15) and (17)] and the Chen and Kareem method is also shown in Fig. 4 for the case of prototypes characterized by the dynamic properties of the Kärkinen and Shanghai bridges.

Furthermore, the accuracy of the proposed method is investigated for the previous prototypes in estimating the onset flutter in the case of zero, moderate, and high structural damping ratios, and is presented in Tables 2 and 3. The proposed solutions are compared with those given by the CEA (Strømmen 2006) and an available simplified approach method (Chen and Kareem 2007). It is noted that the degree of difference between solutions given by the proposed method and the reference approaches depends on the levels of structural damping. More precisely, the accuracy of the proposed simplified approach is inferior when a high structural damping level is used.

Table 2 Result comparisons for R15, 2TF and Flat Plate section using non-dimensional dynamic parameter of $\beta_1 = 0.002$ ($\lambda_z = 0.013, \lambda_\theta = 0.127$)

Damping level	Flutter derivative set	Approx. 1		Approx. 2		Chen's formula		C.E.A	
		V_c^{approx}	f_c^{approx}	V_c^{approx}	f_c^{approx}	V_c^{approx}	f_c^{approx}	V_c	f_c
		(m/s)	(Hz)	(m/s)	(Hz)	(m/s)	(Hz)	(m/s)	(Hz)
$\zeta_z = \zeta_\theta = 0.0\%$	R15	114.587	0.5902	109.999	0.5899	113.112	0.5955	112.372	0.5949
	$\Delta Err(\%)$	1.97	-0.80	-2.11	-0.84	0.66	0.09	-	-
	Flat Plate	127.058	0.5565	-	-	129.388	0.5559	128.519	0.5577
	$\Delta Err(\%)$	-1.14	-0.20	-	-	0.68	-0.32	-	-
	2TF	158.131	0.5525	130.856	0.5545	161.247	0.5511	160.860	0.5508
	$\Delta Err(\%)$	-1.70	0.30	-18.65	0.67	0.24	0.05	-	-
$\zeta_z = \zeta_\theta = 0.5\%$	R15	114.616	0.5902	110.022	0.5899	116.211	0.5870	115.163	0.5886
	$\Delta Err(\%)$	-0.47	0.27	-4.46	0.22	0.91	-0.27	-	-
	Flat Plate	127.096	0.5565	-	-	130.941	0.5513	130.269	0.5549
	$\Delta Err(\%)$	-2.44	0.29	-	-	0.52	-0.65	-	-
	2TF	158.180	0.5525	130.897	0.5545	162.744	0.5476	163.304	0.5486
	$\Delta Err(\%)$	-3.14	0.72	-19.84	1.08	-0.34	-0.17	-	-
$\zeta_z = \zeta_\theta = 1.0\%$	R15	114.704	0.5902	110.093	0.5899	118.505	0.5795	117.482	0.5830
	$\Delta Err(\%)$	-2.37	1.22	-6.29	1.18	0.87	-0.60	-	-
	Flat Plate	127.209	0.5565	-	-	132.401	0.5468	132.030	0.5524
	$\Delta Err(\%)$	-3.65	0.74	-	-	0.28	-1.02	-	-
	2TF	158.329	0.5525	131.020	0.5545	164.224	0.5441	166.400	0.5456
	$\Delta Err(\%)$	-4.85	1.26	-21.26	1.62	-1.31	-0.27	-	-

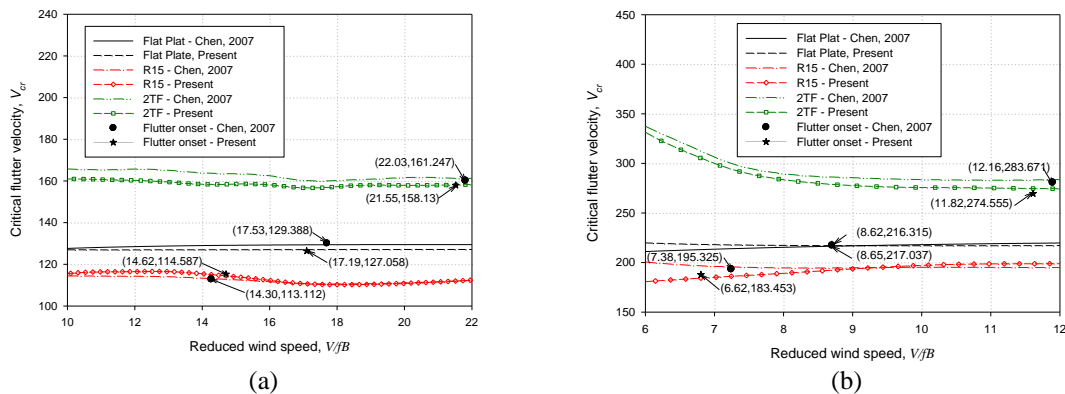


Fig. 4 Comparison critical wind speed results for different deck section: (a) $\beta = 0.002$ and (b) $\beta = 0.082$

Table 3 Result comparisons for R15, 2TF and Flat Plate section using non-dimensional dynamic parameter of $\beta_2 = 0.082(\lambda_z = 0.094, \lambda_\theta = 0.873)$

Damping level	Flutter derivative set	Approx. 1		Approx. 2		Chen's formula		C.E.A	
		V_c^{approx} (m/s)	f_c^{approx} (Hz)	V_c^{approx} (m/s)	f_c^{approx} (Hz)	V_c^{approx} (m/s)	f_c^{approx} (Hz)	V_c (m/s)	f_c (Hz)
$\zeta_z = \zeta_\theta = 0.0\%$	R15	183.453	0.5385	191.757	0.5333	195.325	0.5137	198.474	0.5121
	$\Delta Err(\%)$	-7.57	5.15	-3.38	4.14	-1.59	0.31	-	-
	Flat Plate	217.037	0.4871	-	-	216.315	0.4873	225.192	0.4998
	$\Delta Err(\%)$	-3.62	-0.56	-	-	-3.94	-0.53	-	-
	2TF	274.555	0.4509	230.451	0.4483	284.551	0.4509	293.804	0.4566
	$\Delta Err(\%)$	-6.55	-1.24	-21.56	-1.81	-3.15	-1.23	-	-
$\zeta_z = \zeta_\theta = 0.5\%$	R15	183.469	0.5385	191.711	0.5333	189.905	0.5290	201.494	0.5059
	$\Delta Err(\%)$	-8.95	6.44	-4.86	5.41	-5.75	4.57	-	-
	Flat Plate	217.049	0.4871	-	-	218.679	0.4818	227.775	0.4858
	$\Delta Err(\%)$	-4.71	0.27	-	-	-3.99	-0.83	-	-
	2TF	274.568	0.4509	230.462	0.4483	284.802	0.4504	295.992	0.4551
	$\Delta Err(\%)$	-7.24	-0.92	-22.14	-1.49	-3.78	-1.03	-	-
$\zeta_z = \zeta_\theta = 1.0\%$	R15	183.517	0.5384	191.762	0.5332	201.009	0.4995	204.174	0.5004
	$\Delta Err(\%)$	-10.12	7.61	-6.08	6.57	-1.55	-0.17	-	-
	Flat Plate	217.085	0.4871	-	-	220.774	0.4769	230.195	0.4822
	$\Delta Err(\%)$	-5.69	1.02	-	-	-4.09	-1.10	-	-
	2TF	274.609	0.4509	230.493	0.4483	285.867	0.4481	298.904	0.4517
	$\Delta Err(\%)$	-8.13	-0.18	-22.89	-0.75	-4.36	-0.81	-	-

3. Further simplified formulations

3.1. Based on inter-relationship among uncoupled flutter derivatives

Scanlan and Tomko (1971) presented the expressions of the uncoupled aerodynamic derivatives in terms of circulatory function (Theodorsen 1934) for a thin airfoil. Especially, when the geometric and rotation center are coincident, such as a bridge with its sign convention for the displacements and self-excited forces as shown in Fig. 1, they can be expressed as follows

$$H_1^* = -\frac{\pi}{k} F(k) \quad , \quad H_4^* = \frac{\pi}{2} \left[1 + \frac{2G(k)}{k} \right] \quad (18a,b)$$

$$A_2^* = -\frac{\pi}{16k} \left[1 - F(k) - \frac{2G(k)}{k} \right], \quad A_3^* = \frac{\pi}{8k^2} \left[F(k) - \frac{kG(k)}{2} \right] \quad (19a, b)$$

where $F(k)$ and $G(k)$ are the real and imaginary parts, respectively, of the Theodorsen function. Hence, the flutter derivatives of A_3^* and H_4^* can be found

$$A_3^* = -\left[\left(\frac{4+k^2}{32k} \right) H_1^* + \frac{\pi}{32} \left(\frac{16k}{\pi} A_2^* + 1 \right) \right] \quad (20)$$

$$H_4^* = \frac{\pi}{2} \left[2 + \frac{16k}{\pi} A_2^* + \frac{k}{\pi} H_1^* \right] \quad (21)$$

Eqs. (20) and (21) show the equations for calculating the flutter derivatives A_3^* and H_4^* with respect to the flutter derivatives H_1^* and A_2^* , respectively, for the thin airfoil. It is well known that H_1^* and A_2^* have key roles in describing the aeroelastic behavior for a rectangular section with different chord-to-thickness ratios (Matsumoto 1996). Moreover, Bartoli and Mannini (2008) reported that these aerodynamic derivatives are quite reliable and are the easiest to identify through wind-tunnel tests.

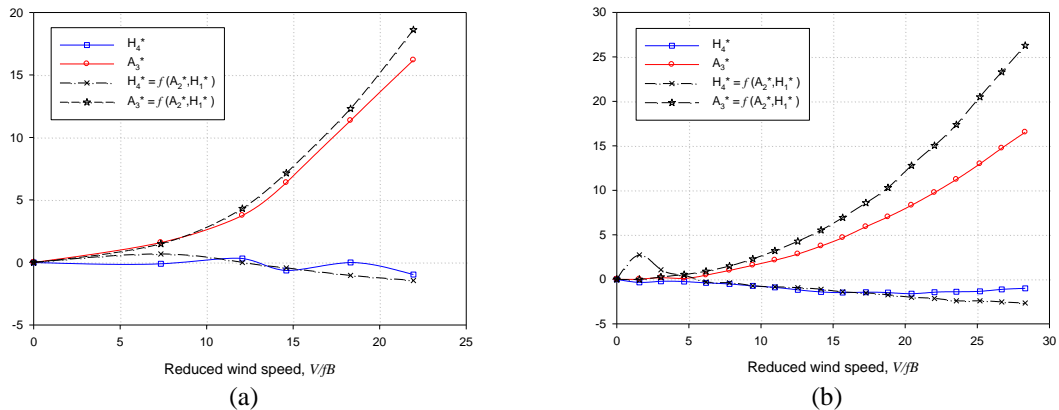


Fig. 5 Degree of approximation of Eqs. (20) and (21) for different deck sections: (a) R15 section and (b) 2TF section

Fig. 5 depicts the approximated degree of A_3^* and H_4^* with those identified through the wind-tunnel test for the rectangular section of R15, and the slotted girder section of 2TF. It is evident that the inter-relationships among uncoupled flutter derivatives, derived from a classical flat plate section, are a good approximation for the section of R15, while they show poor accuracy for the section of 2TF; however, the approximation degree is still acceptable. Thus, Eqs. (20) and (21) associated with Eqs. (15) and (17) can represent further simplified formulations, Approx. 2 for estimating the flutter frequency and reduced wind speed, so that only experimental flutter

derivatives A_2^* and H_1^* are measured from the spring-mounted bridge section model in the wind-tunnel test.

Tables 2 and 3 also illustrate the results obtained by Approx. 2 at the different structural damping levels for the reference prototypes. It is concluded that the approximated solutions for the girder section 2TF are more inferior to those of the rectangular section R15, as expected when compared with those obtained by other methods. Moreover, Approx. 2 provided underestimated solutions compared with those given by the traditional CEA method.

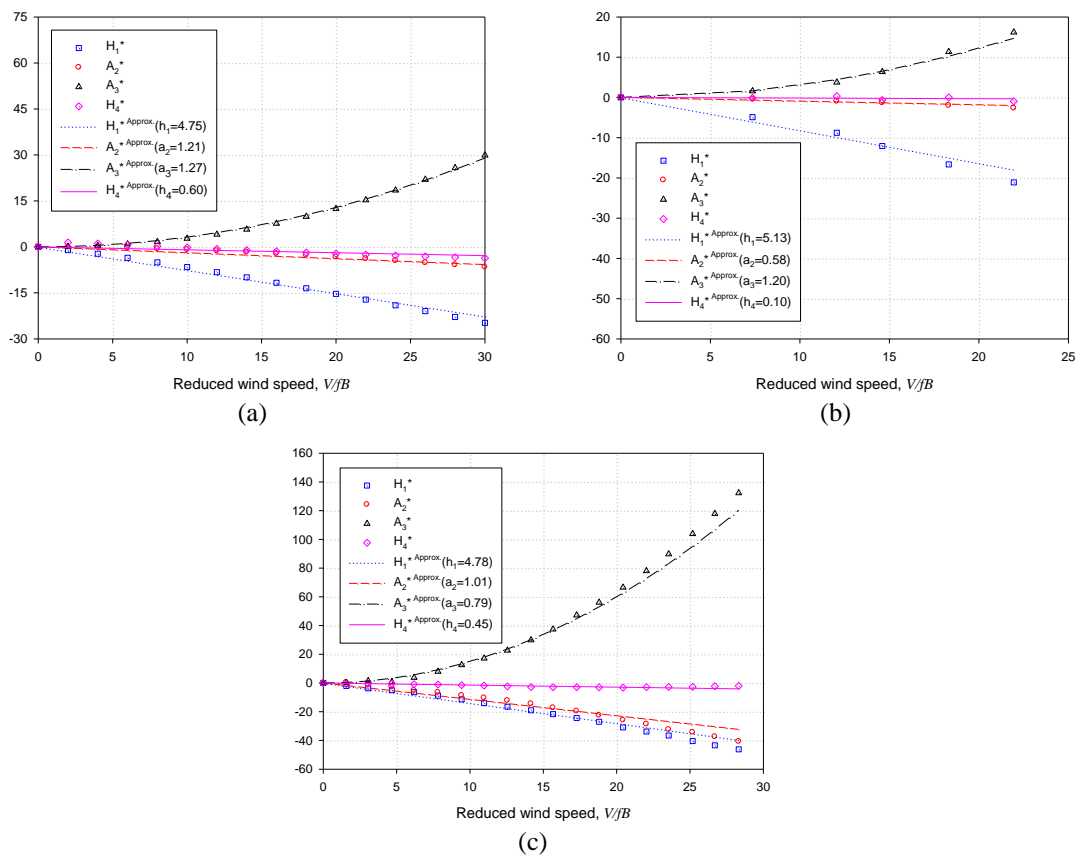


Fig. 6 Degree of approximation of $H_i^{*appr}(i=1,4)$ and $A_i^{*appr}(i=2,3)$ for deck section: (a) Flat Plate, (b) R15 and (c) 2TF

3.2. Based on the quasi stationary approach

Usually, the coupled flutter phenomena encountered in long-span bridges at large wind speeds, where air flow may not be affected by the cross section oscillations, thus the aerodynamic loads produced on the section can be approximately represented by the steady flow, hence the experiment flutter derivatives can be represented by asymptotic expressions with respect to

reduced frequency (Cremona *et al.* 2002). Accordingly, the derivatives H_1^* , H_4^* and A_2^* become proportional to $1/K$, while the derivative A_3^* becomes proportional to $1/K^2$, namely

$$H_1^* \cong H_1^{*approx} = -h_1/K; \quad H_4^* \cong H_4^{*approx} = -h_4/K \quad (22a, b)$$

$$A_2^* \cong A_2^{*approx} = -a_2/K; \quad A_3^* \cong A_3^{*approx} = a_3/K^2 \quad (23a, b)$$

Where h_1, h_4, a_2, a_3 , the positive constants, will be evaluated by inspecting the diagrams of the aerodynamic functions H_1^*, H_4^*, A_2^* and A_3^* , respectively. It is noted that the asymptotic expressions of H_1^*, A_2^* and A_3^* , defined by Eqs. (22(a)), (23(a)) and (23(b)), respectively, are in good agreement with those values obtained by the wind tunnel test for the Normandie, Great Belt East and Akashi bridges (Como *et al.* 2005). Fig. 6 shows the degree of agreement between the experimental values of all the uncoupled flutter derivatives and those obtained by using the asymptotic expressions for the flat plate, *R15* and *2TF* section.

It is further important to observe that if structural damping is neglected in Eq. (15), we obtain the formula of the flutter wind speed as follows

$$V = \omega_\theta B \chi \sqrt{\left(1 - \frac{1}{\gamma^2}\right) \frac{2}{(\lambda_z \lambda_\theta)^{0.5}}} \quad (24)$$

where

$$\chi = \sqrt{\frac{(\lambda_z \lambda_\theta)^{0.5} H_1^* A_2^*}{K^2 (\lambda_z H_1^* + \lambda_\theta A_2^*) (A_3^* H_1^* - A_2^* H_4^*)}} \quad (25)$$

Next, the above asymptotic expansion of the uncoupled flutter derivatives are substituted into Eq. (25), and the assumption of quasi-steady state is then used for Eq. (24), leading to a more simplified formula for predicting the critical wind speed as follows

$$V_{cr} = \lim_{K \rightarrow 0} \left[2\pi f_\theta B g \sqrt{\left(1 - \frac{1}{\gamma^2}\right) \frac{2}{\lambda_z \lambda_\theta}} \right] = \lim_{K \rightarrow 0} \left[2\pi f_\theta B \sqrt{\frac{h_1 a_2 / K^2}{-K^2 (\lambda_z h_1 / K + \lambda_\theta a_2 / K) (a_3 h_1 / K^3 - a_2 h_4 / K^2)}} \sqrt{2 \left(1 - \frac{1}{\gamma^2}\right)} \right] \quad (26)$$

$$V_{cr} = 2\pi f_\theta B \sqrt{\left(1 - \frac{1}{\gamma^2}\right) \frac{2}{a_3 \left(\lambda_z \frac{h_1}{a_2} + \lambda_\theta\right)}} \quad (27)$$

It is observed that Approx. 3, defined by Eq. (27), has a structure similar to the Como's formula, which is derived from simplifying a solution of the continuous model of the suspension bridge motion under the action of the self-excited force, which disregards the role of flutter derivatives of H_4^*, A_4^* .

Eq. (27) shows that the flutter wind speed of the bridge deck section can be immediately predicted by means of mechanical and aerodynamical parameters, and without any iterative

calculations in the reduced frequency domain for the flutter derivatives. It is clear that the vertical damping derivatives H_4^* do not participate in flutter simulation. Thus, this work confirms the key role of flutter derivatives H_1^* , A_2^* and A_3^* for sections that are prone to coupled flutter at large reduced wind speed as reported by the previous researchers (e.g., Como *et al.* 2005, Bartoli and Mannini 2008).

4. Numerical validations

In this section, the assessment accuracy and consistency of the proposed formulas are illustrated. Accordingly, a comparison between the solution of the available methods and that of the proposed formulations is performed for a variety of deck sections that are prone to different types of flutter.

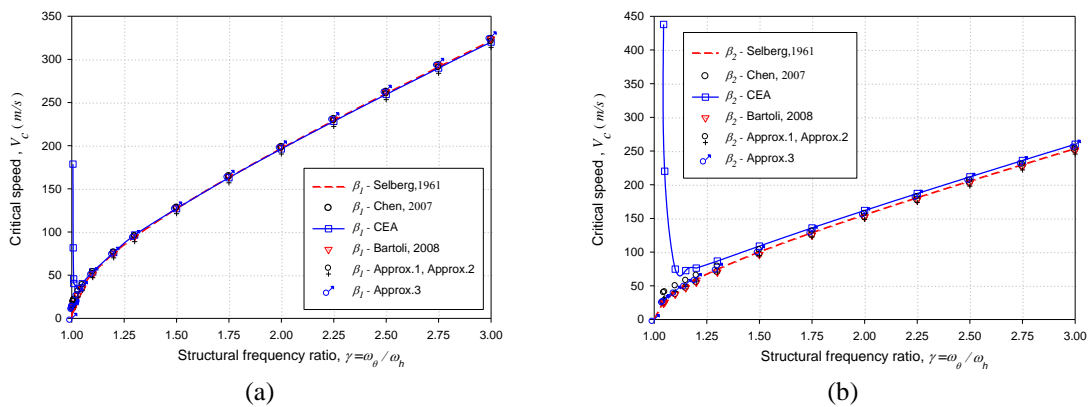


Fig. 7 Comparison on critical wind speed of Flat Plate section at varying frequency ratios: (a) $\beta_1 = 0.002$ and (b) $\beta_2 = 0.082$

4.1. Coupled-mode flutter cases

It is known that the flat plate section and rectangular section of R15 are prone to the coupled-mode flutter. Firstly, a sensitivity analysis of the critical wind speed is carried out at various frequency ratios under zero damping level for the two previous prototypes (Lee *et al.* 2011). Results are illustrated in Fig. 7 for the flat plate section and Fig. 8 for the rectangular section of R15.

The first conclusion drawn from these graphs for the proposed formulas is that they give results that are very close to those obtainable from the solution of the traditional CEA as well as available methods at which the torsional frequency significantly differs from the vertical bending frequency. On the contrary, when the structural frequency ratio tends to unity, neither the approximated formulas nor the empirical formulas and all the adopted benchmark approaches are able to reproduce a sudden increase in flutter critical wind speed as occurs with the traditional CEA approach.

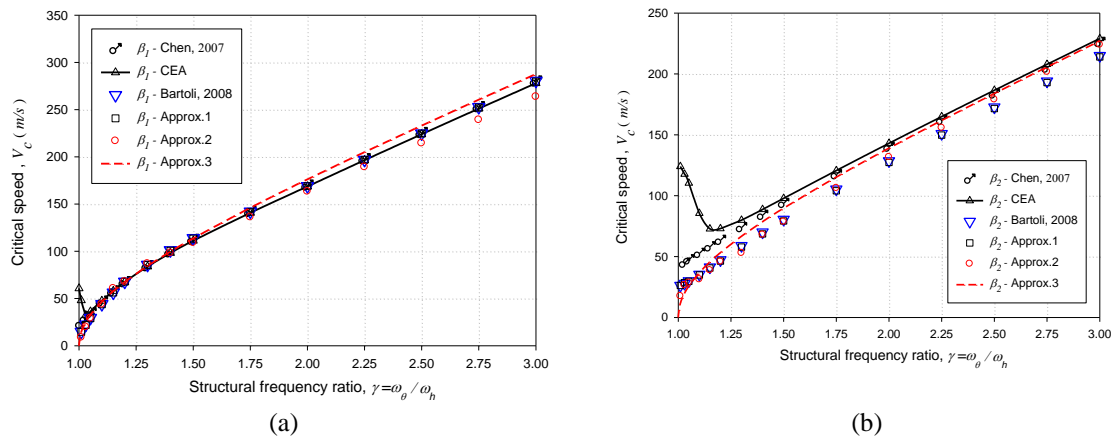


Fig. 8 Comparison on critical wind speed of R15 section at varying frequency ratios: (a) $\beta_1 = 0.002$ and (b) $\beta_2 = 0.082$

It should be noted that if both the coupled and uncoupled flutter derivatives are still fully remained in simplified formulas based on bimodal coupled flutter analysis framework, it may provide reasonable results even if the torsional frequency is close to the vertical bending frequency in the case of low damping (Vu *et al.* 2011).

Fig. 9 plots the critical parameter values of χ_{cr} at the onset flutter given by the Chen and Kareem, and the Approx. 1 and Approx. 2 formulations. It seems that the values of χ_{cr} suddenly increase or decrease as the frequency ratio values become smaller than 1.25 and 1.5 for the prototype assumed by β_1 and β_2 , respectively. Conversely, the values of χ_{cr} seem to be insensitive when the frequency ratio increases beyond that range.

Assuming the parameter β_1 for the flat plate, both the proposed methods of Approx. 1 and Approx. 2 show the critical aerodynamic parameter value of χ_{cr} as 0.412, which is close to that given by the Chen and Kareem method at the range of frequency ratio of $\gamma \geq 1.5$. For the rectangular section of R15, Approx. 2 shows the critical value of χ_{cr} as 0.346, which is about smaller than that given by Approx. 1 and the Chen and Kareem approaches. There is no 4.4% distinction in the critical parameter χ_{cr} when the aerodynamics parameter β_2 is considered.

In addition to validating the accuracy and effectiveness of the proposed approximate approaches, eight case studies are taken into account, three of which that are reported in Table 4 originate from the existing bridges: case study 1 for the 2nd Geo-Germ (Larsen 2002), case study 6 for the Busan- Geoge (Lee *et al.* 2004) and case study 7 for Great Belt (Larsen 1993, Nissen *et al.* 2004). The other case studies are combinations of the dynamic parameters of bridges listed in Table 1 and the flutter derivatives set measured from the cross sections prone to the coupled flutter.

The solution of critical wind speeds and frequencies calculated from the approximated formulations as well as the approximated results calculated from the Chen and Kareem, and the Bartoli and Mannini's formulations, are compared with those of CEA. The evidence from the

available experimental wind tunnel tests in these studies is used as benchmarks. In Table 5, flutter critical conditions (critical wind speed V_c and critical frequency f_c) estimated via present approaches and available reference solutions (or experimental data) are compared.

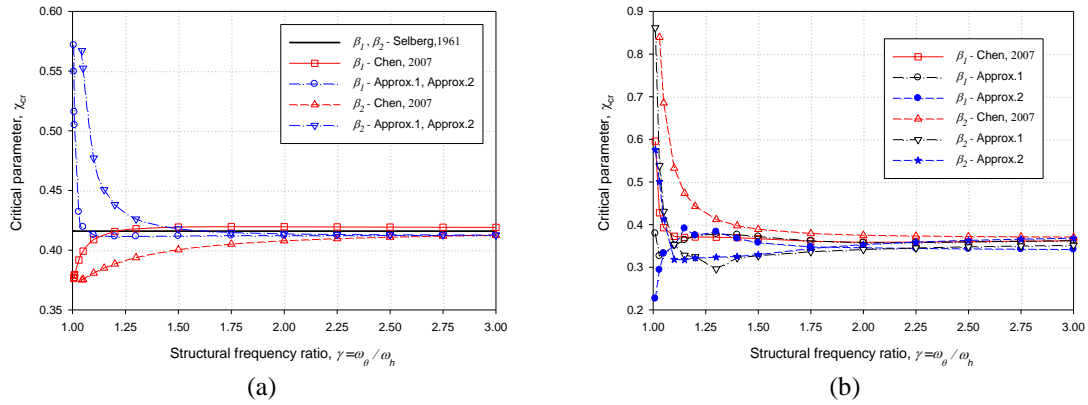


Fig. 9 Comparison on critical parameter χ_{cr} at varying frequency ratios (a) Flat Plate section and (b) R15 section

Table 4 Case study for coupled-mode flutter analysis

Case study	Flutter derivative set	a_3	h_1/a_2	$B(m)$	$f_z (Hz)$	γ	$\zeta_z (\%)$	$\zeta_\theta (\%)$	λ_z	λ_θ
1	2nd Geo-Germ	0.43	13.32	16.9	0.185	2.99	0.30	0.30	0.031	0.345
2	2nd Geo-Germ			34	0.250	1.84	0.50	0.50	0.050	0.606
3	R15	1.20	8.92	13.28	0.465	1.51	0.64	0.64	0.18	0.19
4	2TF	0.79	4.72	36	0.232	2.31	1.00	1.00	0.059	0.525
5	Flat Plate	1.27	3.93	60.4	0.080	1.32	1.00	1.00	0.083	0.594
6	Busan Geoge	1.94	198.26	22	0.334	3.00	0.50	0.50	0.023	0.205
7	Great Belt	0.85	11.11	31	0.099	2.75	0.50	0.50	0.053	0.467
8	Great Belt			51.5	0.252	2.64	0.50	0.50	0.094	0.873

From the results, it can be concluded that the proposed approximate formulas are effective and accurate, resulting in good agreement with the reference solutions in most cases, especially if all uncoupled flutter derivatives (Approx. 1) or only H_1^*, A_2^* and A_3^* (Approx. 3) are considered. In some cases, the results are close to those given by the traditional CEA or agree well with those obtained by the wind tunnel test. The approximated solution in the critical coupling frequency is particularly accurate. However, not only the proposed formulations but also the available approximated formulations, as expected, show inaccurate results when the structural frequency ratio is small and a higher structure damping is used (Case 5 in Tables 4 and 5). It is also consistent with the Bartoli and Manini's research results. Bartoli and Manini (2008) reported that their simplified analytical expressions for critical frequency and reduced wind speed based on flutter

derivatives of H_1^* , A_2^* and A_3^* instead of the usual eight, may provide accurate results of onset flutter when the frequency ratio larger than 1.3. The same results are also observed in Chen and Kareem (2007) method wherein only based only H_3^* , A_1^* , A_2^* and A_3^* flutter derivatives are needed to calculate the onset flutter.

Finally, the approximate formulas that consolidate only the two flutter derivatives of H_1^* and A_2^* (Approx. 2) are less accurate than those adopting four or three uncoupled flutter derivatives; but their accuracy seems to be accepted, since only two cases have large errors (Cases 4 and 6 in Tables 4 and 5).

Table 5 Comparison of critical wind speed results for different deck sections

Analysis methods	Onset flutter error	Case study							
		1	2	3	4	5	6	7	8
Approx.1	$V_c (m/s)$	130.19	175.44	114.64	82.60	24.66	56.87	69.53	206.19
	$f_c (Hz)$	0.4230	0.3434	0.590	0.1623	0.0723	1.0064	0.2125	0.5202
	$\Delta V_c (\%)$	-3.11	1.58	-1.76	-6.67	-22.17	-5.59	-8.41	-1.49
	$\Delta f_c (\%)$	2.79	-5.29	0.97	0.90	1.69	2.20	1.09	-4.47
Approx.2	$V_c (m/s)$	144.53	197.20	110.04	71.96	-	49.01	74.08	249.79
	$f_c (Hz)$	0.4144	0.3449	0.5899	0.1600	-	0.9730	0.2126	0.5164
	$\Delta V_c (\%)$	7.12	12.44	-6.02	-22.44	-	-22.52	-1.76	16.22
	$\Delta f_c (\%)$	0.75	-4.83	0.93	-0.49	-	-1.15	1.12	-5.24
Approx.3	$V_c (m/s)$	138.61	158.36	114.01	83.91	25.67	61.47	73.68	220.51
	$\Delta V_c (\%)$	3.15	-9.04	-2.32	-5.00	-17.37	2.31	-2.31	5.10
Chen's forms	$V_c (m/s)$	149.75	179.31	116.92	86.08	24.78	57.67	77.61	210.94
	$f_c (Hz)$	0.4540	0.3900	0.5848	0.1601	0.0713	1.0030	0.2047	0.5310
	$\Delta V_c (\%)$	10.36	3.71	0.23	-2.36	-21.58	-4.14	2.88	0.79
	$\Delta f_c (\%)$	9.42	7.30	0.07	-0.44	0.35	1.87	-2.68	-2.35
Bartoli's forms	$V_c (m/s)$	134.64	186.08	119.51	86.97	24.74	60.90	72.74	199.06
	$f_c (Hz)$	0.4190	0.3435	0.5870	0.1608	0.0713	0.9858	0.2113	0.5404
	$\Delta V_c (\%)$	0.30	7.21	2.39	-1.31	-21.76	1.39	-3.63	-5.13
	$\Delta f_c (\%)$	1.85	-5.24	0.43	-0.01	0.39	0.16	0.49	-0.55
CEA	$V_c (m/s)$	134.24	172.67	116.66	88.11	30.13	60.05	75.38	209.27
	$f_c (Hz)$	0.4112	0.3615	0.584	0.1608	0.0711	0.9843	0.2102	0.5434
Wind tunnel test	$V_c (m/s)$	140.46	-	-	-	-	61.80	74.30	-

4.2. Single-mode flutter cases

4.2.1. Torsional flutter

If a bluff cross section has values of A_2^* and tends to change its sign from negative to positive causing negative aerodynamic damping, the section is prone to torsional flutter. In this case, a well-known simplified method to deal with that flutter type involves performing a mode-by-mode analysis by neglecting modal coupling (Simiu and Scanlan 1996, Strømmen 2006). Accordingly, the solution can be determined from the combination of the following equations, which are reported here with the notation adopted in the present paper

$$1 + \frac{\rho B^4}{2\tilde{m}_\theta} A_3^*(K) - \frac{1}{\Omega^2} = 0 \tag{28}$$

$$\zeta_\theta - \Omega \frac{\rho B^4}{4\tilde{m}_\theta} A_2^*(K) = 0 \tag{29}$$

In order to validate the degree of approximation of the proposed formulas for the cross sections that are prone to torsional flutter, let us consider two previous reference sections characterized by the aerodynamic properties of a rectangular cylinder $R5$ with width to depth ratios of 5 (Matsumoto 1996) with fundamental torsional frequencies of 0.7012 (Hz) and 0.6650 (Hz), respectively. In Fig. 10, the critical reduced wind speed solutions obtained by CEA, 1-DOF Torsion formulation [Eqs. (28) and (29)] and the proposed formulas are plotted against the frequency ratio under zero damping level.

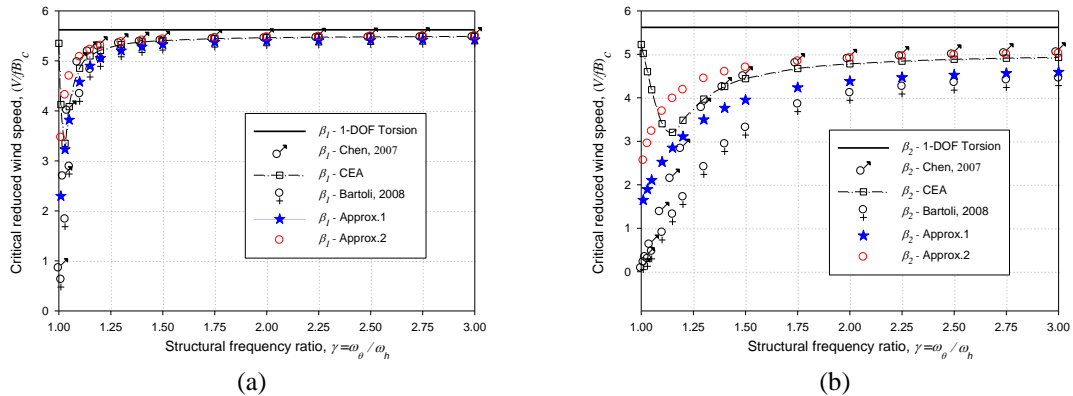


Fig. 10 Comparison on critical reduced wind speed of $R5$ section at varying frequency ratios: (a) $\beta_1 = 0.002$ and (b) $\beta_2 = 0.082$

It is observed that the 1-DOF Torsion formulation still gives constant values for the critical reduced wind speed solution when the structural frequency ratio is changed. However, when natural torsional and flexural frequencies tend to coincide, the flutter critical wind speed given by the proposed formulas significantly reduces. Furthermore, at the range where γ is greater than

1.25, it is worth noting that a very good agreement between these approaches occurs when the non-dimension parameter β_1 is assumed. Meanwhile, there is a slight variance in solutions calculated by the proposed and reference methods, which can be observed in Fig. 10 for the case of β_2 .

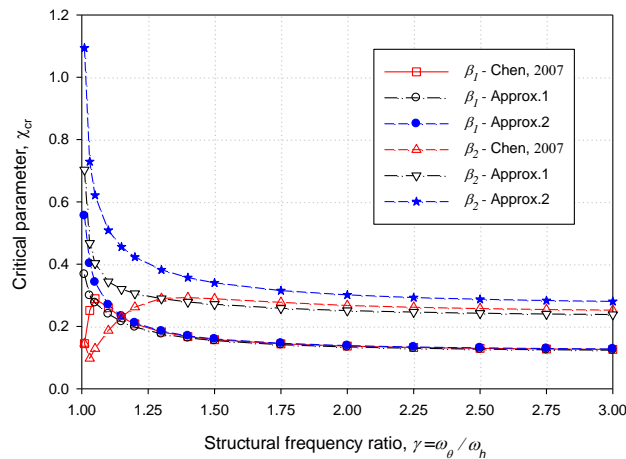


Fig. 11 Comparison on parameter χ_{cr} of R5 section at varying frequency ratios

Fig. 11 illustrates the sensitive analysis in the critical parameter value of χ_{cr} given by the Chen and Kareem method and the Approx. 1 and Approx. 2 formulations for the rectangular cylinder R5. It is noted that the proposed formulas and the Chen and Kareem formula can be adequate to give a value of χ_{cr} between 0.18 and 0.12, when the frequency ratio, γ , varies from 1.5 to 3.0 for the prototype characterized by the non-dimension parameter of β_1 . Meanwhile, assuming β_2 for the prototype, an increase of up to 47% and 49% in the critical parameter χ_{cr} obtained by Approx. 1, and the Chen and Kareem approach is observed, respectively. On the other hand, these approaches show critical values of χ_{cr} that are lower than those given by the Approx. 2 approach.

Further numerical validation of the case studies is presented in Table 6, in which one case study of the existing structure, the Seohae Grand Bridge (Case 5) is shown. The other case studies are prototypes combined with the geometric parameters of the existing bridges such as Busan-Geoge (Case1, Case 3), Kärkinen (Case 2, Case 4), Messina Straits (Case 6) and the aerodynamics parameters of R5 and the rectangular section of R10 with width to depth ratios of 10 (Matsumoto 1996). Table 7 reports the values of flutter onset computed for a number of case studies listed in Table 6. It seems possible to conclude that the proposed formulas give results that agree well with those of CEA or the reference approximated methods. However, for the case characterized by a small frequency ratio, the proposed Approx. 2 formulas show poor accuracy results when compared with those of the other methods (Case 6 in Tables 6 and 7).

Table 6 Case study of torsional flutter analysis

Case study	Flutter derivative set	$B(m)$	$f_z(Hz)$	γ	$\zeta_z(\%)$	$\zeta_\theta(\%)$	λ_z	λ_θ
1	R5	22	0.334	3.00	0.5	0.5	0.023	0.205
2	R5	13.28	0.465	1.51	0.64	0.64	0.013	0.127
3	R10	22	0.334	3.00	0.5	0.5	0.023	0.205
4	R10	13.28	0.465	1.51	0.64	0.64	0.013	0.127
5	Seohae Grand	34	0.250	1.84	0.5	0.5	0.050	0.606
6	Seohae Grand	60.4	0.061	1.32	1.00	1.00	0.083	0.594

Table 7 Comparison of critical wind speed and frequency results for different deck sections prone to torsional flutter

Analysis methods	Onset flutter error	Case study					
		1	2	3	4	5	6
Approx.1	$V_c(m/s)$	109.19	47.44	158.19	69.30	47.56	14.05
	$f_c(Hz)$	0.9328	0.6696	0.9098	0.6585	0.4294	0.0730
	$\Delta V_c(\%)$	-5.89	-9.69	-6.40	-10.46	-3.25	-8.78
	$\Delta f_c(\%)$	0.59	0.49	0.85	0.94	2.20	-0.22
Approx.2	$V_c(m/s)$	114.05	49.07	159.66	69.84	46.84	11.46
	$f_c(Hz)$	0.9558	0.6801	0.9129	0.6599	0.3935	0.0675
	$\Delta V_c(\%)$	-1.70	-6.60	-5.53	-9.75	-4.71	-25.64
	$\Delta f_c(\%)$	3.08	2.06	1.20	1.16	-6.36	-7.73
1-DOF Torsion forms	$V_c(m/s)$	118.95	54.53	179.84	85.19	52.52	16.65
	$f_c(Hz)$	0.9121	0.6616	0.8535	0.6327	0.4110	0.0712
	$\Delta V_c(\%)$	2.52	3.79	6.41	10.08	6.84	8.03
	$\Delta f_c(\%)$	-1.63	-0.71	-5.39	-3.02	-2.20	-2.69
Chen's forms	$V_c(m/s)$	117.70	53.68	169.56	77.61	51.88	15.99
	$f_c(Hz)$	0.9270	0.6660	0.8983	0.6520	0.4600	0.0796
	$\Delta V_c(\%)$	1.44	2.18	0.33	0.27	5.53	3.80
	$\Delta f_c(\%)$	-0.02	-0.05	-0.42	-0.06	9.47	8.83
Bartoli's forms	$V_c(m/s)$	113.27	52.04	165.88	76.96	48.23	15.23
	$f_c(Hz)$	0.9306	0.6712	0.9069	0.6580	0.4275	0.0749
	$\Delta V_c(\%)$	-2.37	-0.94	-1.85	-0.56	-1.88	-1.18
	$\Delta f_c(\%)$	0.36	0.73	0.54	0.86	1.75	2.42
CEA	$V_c(m/s)$	116.02	52.54	169.01	77.39	47.55	15.41
	$f_c(Hz)$	0.9273	0.6663	0.9021	0.6524	0.4210	0.0731

4.2.2. Heaving-mode aeroelastic instability

A similar procedure can be used for the instability dominated by a heaving mode (i.e., galloping type) of a cross section having values of H_1^* that tend to change the sign of the cross section from negative to positive. In this case, the solution is obtained by solving the combined equations as follows (Simiu and Scanlan 1996, Strømmen 2006)

$$\zeta_z - \Omega \frac{\rho B^2 \gamma}{4 \tilde{m}_\theta} H_1^*(K) = 0 \tag{30}$$

$$1 + \frac{\rho B^2}{2 \tilde{m}_z} H_4^*(K) - \frac{1}{\gamma^2 \Omega^2} = 0 \tag{31}$$

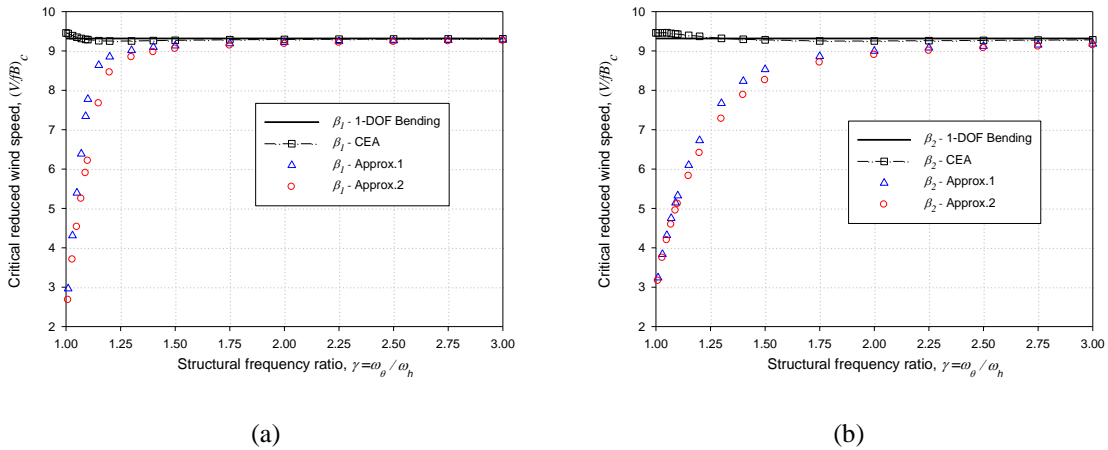


Fig. 12 Comparison on critical reduced wind speed of c section at varying frequency ratios: (a) $\beta_1=0.002$ and (b) $\beta_2 = 0.082$

Fig. 12 depicts the critical reduced wind speed of the previous prototypes versus the structural frequency ratio γ . These prototypes use aerodynamics properties of a rectangular cylinder $R1$ with width to depth ratios of 1 (Matsumoto 1996) that are prone to heaving-mode aeroelastic instability when the fundamental vertical frequencies are 0.4646 (Hz) and 0.2520 (Hz), respectively. Results obtained via the present formulations are compared with the numerical solutions given by the 1-DOF Bending formulation [Eqs. (30) and (31)] and CEA. It can be noted that the proposed approaches give results which are in good agreement with the reference solutions, especially for the prototype characterized by β_1 when $\gamma > 1.5$.

Fig. 13 shows a comparison of the critical parameter value of χ_{cr} given by the proposed approaches. For the prototype characterized by β_2 , it can be noted that both the Approx. 1 and Approx. 2 methods show that the value of the critical parameter χ_{cr} , which is slightly sensitive to the frequency ratio, varied from 0.07 to 0.13 at a range of frequency ratio $\gamma = 1.25 - 3.0$. However,

there is a larger discrepancy in χ_{cr} for the prototype characterized by β_2 .

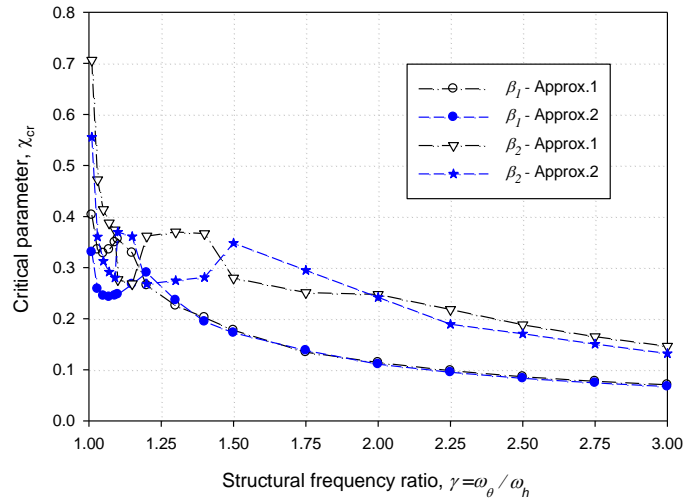


Fig. 13 Comparison on critical parameter χ_{cr} of R1 section at varying frequency ratios

Table 8 shows that the case studies of the prototypes that are combined the geometric parameters of the previous bridge is listed in Table 1, with using the flutter derivative set of R1, R2 are rectangular prisms with $B/D = 1,2$ (Matsumoto 1996), and the Deer Isle bridge (Caracoglia and Jones 2003), which has heaving divergent type instability. Table 9 summarizes the results of the critical reduced velocity and frequency using the proposed formulas and reference methods.

From the results, it can be concluded that the proposed formula, Approx. 1 gives satisfactory results when compared with the adopted benchmark approaches in most cases (with the exception of Cases 4 and 5 in Tables 8 and 9). Meanwhile, it can be seen that the accuracy of the proposed Approx. 2 formulation, in which only two experimental flutter derivatives are adopted, is inferior to those reference methods but the degree of approximation seems to still be acceptable.

Table 8 Case study of vertical flutter analysis

Case study	Flutter derivative set	$B(m)$	$f_z (Hz)$	γ	$\zeta_z (\%)$	$\zeta_{\theta} (\%)$	λ_z	λ_{θ}
1	R1	22	0.334	3.00	0.50	0.50	0.023	0.205
2	R1	13.28	0.465	1.51	0.64	0.64	0.013	0.127
3	R2	13.28	0.465	1.51	0.64	0.64	0.013	0.127
4	R2	60.4	0.061	1.32	1.00	1.00	0.083	0.594
5	Deer Isle	60.4	0.061	1.32	1.00	1.00	0.083	0.594
6	Deer Isle	34	0.250	1.84	0.50	0.50	0.050	0.606

Table 9 Comparison of critical wind speed and frequency results for different deck sections prone to vertical flutter

Analysis methods	Onset flutter error	Case study					
		1	2	3	4	5	6
Approx.1	$V_c (m/s)$	61.48	54.05	58.34	22.97	13.09	28.08
	$f_c (Hz)$	0.3017	0.4456	0.4048	0.0358	0.0737	0.2736
	$\Delta V_c (\%)$	-4.87	-3.46	-4.76	-11.56	15.35	2.27
	$\Delta f_c (\%)$	-3.84	-0.81	-2.21	-6.93	11.37	3.28
Approx.2	$V_c (m/s)$	57.34	52.17	58.34	29.03	10.13	23.44
	$f_c (Hz)$	0.2823	0.4346	0.4048	0.0335	0.0821	0.2527
	$\Delta V_c (\%)$	-11.27	-6.83	-4.87	11.80	-10.75	-14.61
	$\Delta f_c (\%)$	-10.03	-3.26	-2.06	-12.98	23.96	-4.60
1-DOF Bending forms	$V_c (m/s)$	63.96	55.84	56.35	27.13	11.49	26.18
	$f_c (Hz)$	0.3105	0.4463	0.3911	0.0369	0.0647	0.2607
	$\Delta V_c (\%)$	-1.02	-0.26	-8.07	4.46	1.25	-4.63
	$\Delta f_c (\%)$	-1.06	-0.65	-5.26	-4.08	-2.28	-1.59
CEA	$V_c (m/s)$	64.62	55.99	61.25	25.97	11.35	27.46
	$f_c (Hz)$	0.3138	0.4492	0.4139	0.0385	0.0662	0.2649

5. Conclusions

Based on the simplified framework of a bimodal flutter problem, the proposed method represents an extension of Selberg's empirical formula to generic bridge sections that may be prone to arbitrary types of aerodynamic instability such as coupled-mode or single-mode (either dominated by torsion or heaving mode) flutter. The pragmatic feature of the proposed method is that only uncoupled flutter derivatives are required to perform the flutter analysis. The proposed formula is still applicable when the relationships among uncoupled flutter derivatives can be used so that only two experimental flutter derivatives of (H_1^*, A_2^*) are measured. Nevertheless, the Approx-2 formula employed the reduction of the flutter derivatives based on the behavior of the thin airfoil and therefore may be less effective for real cross section such as twin-box girder.

The proposed method also provides an aerodynamic index for describing the flutter performance of a given bridge deck section, offering an aerodynamic investigation of the various cross sections.

Moreover, when the quasi-steady state is assumed and the asymptotic expansion of the uncoupled flutter derivatives can be employed, a non-iterative calculated method is able to be applied for the uncoupled flutter derivative in order to predict the critical wind velocity for

long-span bridges that are prone to coupled-mode flutter at large reduced wind speeds.

Finally, from the wind-structure stability analyses carried out on several cases which were widely employed from existing ideal cable-stayed bridges, the present simplified approaches show satisfactory results with the reference solutions, unless the frequency ratio is very close to unity and the structural damping is high level. Thus, proposed simplified formulas could be considered as one of the useful engineering tools for the aeroelastic stability analysis of long-span bridges at the preliminary design stage.

References

- Bartoli, G. and Mannini, C. (2008), "A simplified approach to bridge deck flutter", *J. Wind Eng. Ind. Aerod.*, **96**(2), 229-256.
- Bleich, F. (1949), "Dynamic instability of truss-stiffened suspension bridge under wind action", *Proc. ASCE*, **74**(8), 1269-1314.
- Caracoglia, L. and Jones, N.P. (2003), "Time domain vs. frequency domain characterization of aeroelastic forces for bridge deck sections", *J. Wind Eng. Ind. Aerod.*, **91**(3), 371-402
- Como, M., Del Ferraro S. and Grimaldi, A. (2005), "A parametric analysis of the flutter instability for long span suspension bridges", *Wind Struct.*, **8**(1), 1-12.
- Chen, X. and Kareem, A. (2007), "Improved understanding of bimodal coupled bridge flutter based on closed-form solutions", *J. Struct. Eng. - ASCE*, **133**(1), 22-31.
- Cremona, C. and Foucriat, J.C. (2002), *Comportement au vent des ponts*, Association Francaise de Génie Civil. Paris: Presses de L'Ecole Nationale des Ponts et Chaussées.
- D'Asdia, P. and Sepe, V. (1998), "Aeroelastic instability of long span suspended bridges: a multimode approach", *J. Wind Eng. Ind. Aerod.*, **74-76**, 849-857.
- Dyrbye, C. and Hansen, S.O. (1997), *Wind loads on structures*, Wiley, New York.
- Fung, Y.C. (1993), *An introduction to the theory of aeroelasticity*, Dover Publications Inc., New York.
- Korea Highway Corporation (KHC) (1998), *Wind tunnel report for the Seohae Grand bridge*, Kyunggi-do, Korea.
- Kiviluoma, R. (2001), *Frequency-domain approach for calculating wind induced vibration and aeroelastic stability characteristics of long span bridges*, PhD thesis, Acta Polytechnica Scandinavica.
- Larsen, A. (1993), "Aerodynamic aspects of the final design of the 1624m suspension bridge across the Great Belt", *J. Wind Eng. Ind. Aerod.*, **48**(2-3), 261-285.
- Larsen S.V.(2002), *Section model tests for the design of the 2nd Geo-Germ Bridge*, Force Technology-DMI, Lyngby, Denmark.
- Lee, H.E. et al. (2004), *Section model tests for the design of the cable stayed bridge, Lot1, Busan-Geoge Fixed Link*, Korea University Research Centre for Disaster Prevention Science and Technology, Seoul, Korea.
- Lee, H.E., Vu, T.Y., Yoo, S.Y. and Lee, H.Y. (2011), "A simplified evaluation in critical frequency and wind speed to bridge deck flutter", *Procedia Eng.*, **14**, 1784-1790.
- Livesey, F.M. (1995), *Wind tunnel studies of the Hoga Kusten Bridge during construction*, Part II: Aeroelastic model tests, DMI Report 94124, Danish Maritime Institute, Denmark.
- Matsumoto, M. (1996), "Aerodynamic damping of prisms", *J. Wind Eng. Ind. Aerod.*, **59**(2-3), 159-175
- Matsumoto, M., Shijo, S., Eguchi, A., Hikida, T., Tamaki, H. and Mizuno, K. (2004), "On the flutter characteristics of separated two box girders", *Wind Struct.*, **7**(4), 281-291.
- Nissen, H.D., Sørensen, P.H. and Jannerup, J. (2004), "Active aerodynamic stabilisation of long suspension bridges", *J. Wind Eng. Ind. Aerod.*, **92**(10), 829-847.
- Rocard, Y. (1963), *Instabilité des Ponts Suspendus dans le Vent-Experiences sur Modele Réduit*, Nat. Phys. Lab. Paper 10, England.

- Scott, R. (2001), *In the wake of Tacoma, Suspension Bridges and the Quest for Aerodynamics Stability*, American Society of Civil Engineers, Reston VA.
- Selberg, A. (1961), "Oscillation and aerodynamic stability of suspension bridges", *Acta. Polytech. Scand.*, **13**, 308-377
- Scanlan, R.H. and Tomko, A. (1971), "Airfoil and bridge deck flutter derivatives", *J. Eng. Mech – ASCE*, **97**(EM6), 1717-1737.
- Strømmen, E. (2006), *Theory of bridge aerodynamics*, Springer. Verla Publications.
- Simiu, E. and Scanlan, R.H. (1996), *Wind effects on structures*, Wiley, New York.
- Theodorsen, T. (1934), *General theory of aerodynamic instability and the mechanism of flutter*, Technical Report, 496, N.A.C.A., Washington.
- Vu, T.V, Lee, H.E., Kim, Y.M. and Han, T.S. (2011), "Simplified formulations for flutter instability analysis of bridge deck", *Wind Struct.*, **14**(4), 359-381.
- Yang, Y.X., Ge, Y.J. and Cao, F.C. (2007),"Flutter performance of central-slotted box girder section for Long span suspension Bridges", *China J. Highway Transport*, **20**(3), 35-40.
- Zhou, L. and Ge, Y.J., (2009),"Sectional model test study on vortex-excited resonance of vehicle-bridge system of Shanghai Bridge over Yangtse River", *Frontiers Arch.Civil Eng. China*, **3**(1), 67-72.